Tailoring of Interfacial Mechanical Shear Strength by Surface Chemical Modification of Silicon Microwires Embedded in Nafion Membranes

Betar M. Gallant,[†,§] X. Wendy Gu,[‡] David Z. Chen,[‡] Julia R. Greer,[*,‡,§] and Nathan S. Lewis[*,†,§,∥]

[†]Division of Chemistry and Chemical Engineering, [‡]Division of Engineering and Applied Sciences, [§]The Kavli Nanoscience Institute at Caltech, and [∥]The Beckman Institute at Caltech, California Institute of Technology, Pasadena, California 91125, United States

ABSTRACT The interfacial shear strength between Si microwires and a Nafion membrane has been tailored through surface functionalization of the Si. Acidic (—COOH-terminated) or basic ($—NH_2$-terminated) surface-bound functionality was introduced by hydrosilylation reactions to probe the interactions between the functionalized Si microwires and hydrophilic ionically charged sites in the Nafion polymeric side chains. Surfaces functionalized with SiO_x, Si—H, or $Si—CH_3$ were also synthesized and investigated. The interfacial shear strength between the functionalized Si microwire surfaces and the Nafion matrix was quantified by uniaxial wire pull-out experiments in an *in situ* nanomechanical instrument that allowed simultaneous collection of mechanical data and visualization of the deformation process. In this process, an axial load was applied to the custom-shaped top portions of individual wires until debonding occurred from the Nafion matrix. The shear strength obtained from the nanomechanical measurements correlated with the chemical bond strength and the functionalization density of the molecular layer, with values ranging from 7 MPa for $Si—CH_3$ surfaces to ~16—20 MPa for oxygen-containing surface functionalities. Hence surface chemical control can be used to influence the mechanical adhesion forces at a Si—Nafion interface.

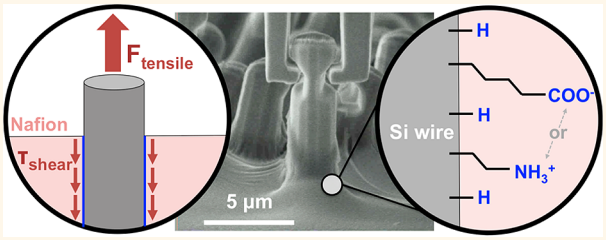

KEYWORDS: Si microwires · *in situ* tension · nanomechanical · surface functionalization · Nafion

Tailoring mechanical adhesion at Si/polymer interfaces is important for the fabrication of a range of devices including stretchable electronics,[1] chemical and optical sensors,[2] light-emitting diodes,[3] microfluidics,[4] and photovoltaic/photoelectrochemical systems.[5−8] In particular, structured Si constituents, such as microwires, embedded in an ionomer (*e.g.*, Nafion) membrane have been investigated as a promising configuration for freestanding solar-driven water-splitting devices.[7,8] In such a scheme, Si microwires function as light-absorbing and electrode constituents, whereas the membrane acts as a physical barrier to integrate the electrodes and separate the gaseous products, while permitting facile ion transport to minimize any pH gradients that will otherwise result from the electrochemical reactions involved in water splitting. Although the bulk mechanical properties of individual constituents of these devices have been widely investigated, the presence of a chemically and mechanically discontinuous interface in composite devices introduces important considerations due to stress concentration. These concerns are particularly acute for flexible photoelectrochemical devices exposed to a range of operational loads including mechanical bending, stretching, and swelling during fabrication or operation.

Mechanical adhesion at interfaces arises fundamentally from molecular interactions; however, the link between molecular-scale chemical properties and macroscopic mechanical behavior is difficult to probe at an inherently buried interface.[9] Peel tests[5,10] are commonly employed but can be limited by poorly defined geometries of deformation. Hence, peel tests provide qualitative observations[10] or absolute force measurements that are not readily generalizable among studies. Atomic-force contact

* Address correspondence to nslewis@caltech.edu, jrgreer@caltech.edu.

Received for review January 21, 2015 and accepted April 14, 2015.

Published online April 14, 2015
10.1021/acsnano.5b00468

measurements enable quantification of molecular-scale interactions,[11,12] but the surfaces interrogated by this method may not be chemically analogous to those formed at buried interfaces. Hence, methods are needed that can address these limitations by combining submicroscale force measurements and well-defined interaction areas, with geometries and fabrication conditions that are relevant to real device applications.

Adhesion between polymers and disparate hard surfaces is commonly manipulated macroscopically by mechanical methods such as reactive etching to increase the surface roughness of the hard substrate.[13] Chemical functionalization methods have also been used; for example, plasma pretreatment of polymer[14] or substrate surfaces has been utilized to introduce polar surface terminations for preferential bonding, although this method suffers from limited surface chemical and structural control. Molecular linkers such as silane coupling agents between metals and polymers[15] or polymer-analogue precursors on transparent conductive oxides[5] have been utilized.[10] However, when used with Si, these strategies typically employ, or result in, oxidized surfaces that are not well-suited for applications[16] wherein device performance depends upon the electronic or chemical quality of the surface.

We describe herein the nature of the chemical interactions at functionalized Si wire array−ionomer interfaces investigated using a custom *in situ* nanomechanical test methodology. The nanomechanical tests have allowed measurement of the variations of the interfacial shear strength for differently chemically functionalized Si microwires embedded in Nafion membranes[17−20] while observing their loading and deformation geometries in real time, a unique advantage of *in situ* testing that allows direct correlation between structural changes and the corresponding load data at the point those changes occurred. This particular composite geometry was used because vertically aligned, pitch-controlled arrays of wires present a well-defined wire spacing and wire contact area with the polymer for measurements of shear stress. An additional advantage of the nanomechanical aspect of this test methodology is the measurement of component materials in the configuration and geometries in which they would be actually used in a photovoltaic or photoelectrochemical water-splitting/fuel-generating device, where the use of nano- and microscale light-absorbing constituents can have important functional advantages.[8,18,19] Nafion, an ionomer consisting of a hydrophobic polytetrafluoroethylene (PTFE) backbone, hydrophilic side chains, and terminal acidic (HSO_3) sites,[20−22] presents several possible moieties for chemical interaction. Si microwire surfaces were therefore modified to probe different predicted interaction strengths[23] *via* relatively weakly interacting van der Waals interactions (0.1−10 kJ mol^{-1}), hydrogen bonding (10−40 kJ mol^{-1}), or electrostatic interactions (∼15 kJ mol^{-1})[24] by functionalization with hydrophobic (Si−CH_3), acidic (SiO_x, Si−$(CH_2)_{10}$COOH), and basic (Si−$(CH_2)_4NH_2$) surface-attached moieties, respectively. The Si−H interactions with Nafion were also measured to investigate the stability of such surfaces in contact with the polymer precursor during processing. The interfacial adhesion between individual functionalized wires and the polymer was measured by loading the wires uniaxially until they debonded from the Nafion matrix,[25] from which the surface-chemistry-dependent maximum shear stress sustained in the molecular interlayer was determined quantitatively.

RESULTS

Acid- or base-terminated, ω-unsaturated olefins[26,27] were attached *via* UV hydrosilylation to planar Si(111) surfaces to evaluate the success of molecular attachment and determine appropriate chemical conditions prior to functionalization of wire arrays. It is noted that microwires, which are grown from a (111)-oriented Si wafer, consist of various facets such as (110) or (211) surfaces[28] and may exhibit moderately different reaction kinetics below saturation coverage. The (111)-oriented Si wafers were first H-terminated by immersion for 30 s into buffered HF(aq), followed by UV (254 nm)-initiated hydrosilylation functionalization under N_2(g) for up to 5 h in a solution of molecular precursors (undecylenic acid or butoxycarbonyl (Boc)-aminobutene, 10% in toluene, Figure 1). An X-ray photoelectron spectroscopic (XPS) high-resolution survey in the C 1s region for undecylenic acid-reacted surfaces revealed that soaking a H−Si(111) wafer in the reaction solution yielded no significant molecular attachment (Figure 2a). However, after a 3 h reaction time with illumination, an increase in sp^3 C−C peak intensity at 285.0 eV, combined with the emergence of a peak at 289.9 eV ascribable to the oxidized carbon in −COOH groups,[29] supported the anchoring of undecanoic acid onto the Si(111) surface. An additional increase in the XPS signal intensity was observed for up to 5 h of reaction time. XPS signals ascribable to SiO_x were not observed even for the longest reactions times (Supporting Information Figure S1), indicating that the oxygen in the −COOH groups did not attack the Si−H surface prior to reaction *via* the olefin end of the molecule. This behavior is consistent with prior reports of similar hydrosilylation reactions.[29−32] The Si−undecanoic acid surfaces appeared to be relatively stable, with no detectable oxidation observed in the XPS Si 2p region after 1 week in air (Figure S2).

The molecular configuration of the undecanoic acid groups on the Si(111) surface was further confirmed by transmission Fourier transform infrared (FTIR) spectroscopy of a 3 h functionalized surface, referenced to the original Si−H background of the same sample prior to

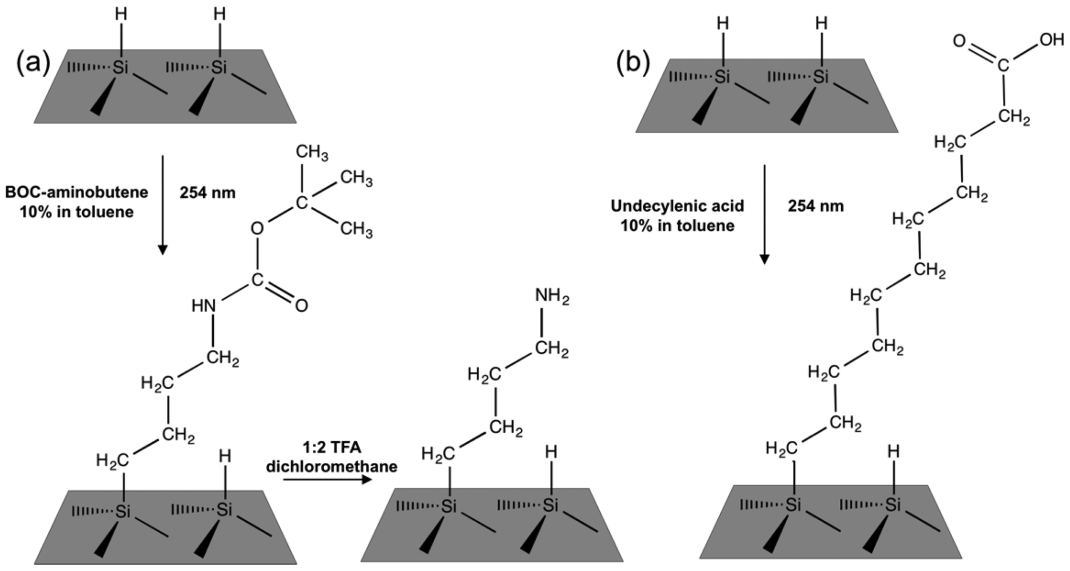

Figure 1. Functionalization scheme for UV hydrosilylation reactions (254 nm) on H-terminated Si(111) and Si microwire surfaces. (a) Reaction of butyloxycarbonyl-protected aminobutene in toluene, followed by subsequent deprotection in trifluoroacetic acid. (b) Reaction of undecylenic acid in toluene.

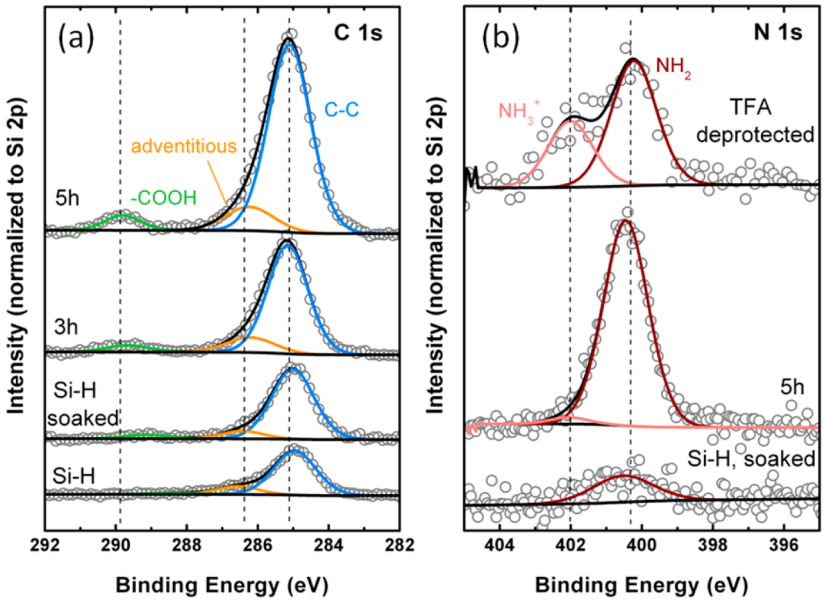

Figure 2. XPS data for Si(111) surfaces functionalized with ω-unsaturated olefins *via* UV hydrosilylation (254 nm). (a) C 1s spectra as a function of reaction time for functionalization with undecylenic acid to yield Si(111)−$(CH_2)_{10}$COOH (undecanoic acid) surfaces and comparison with as-prepared and soaked (overnight, no light) hydride-terminated (Si−H) samples. (b) N 1s spectra for a 5 h reaction time of Si(111) with 1-(Boc-amino)-3-butene, subsequent deprotection with TFA to yield Si(111)−$(CH_2)_4NH_2$ (aminobutane) surfaces, and comparison with a soaked Si−H sample (overnight, no light). All spectra were normalized to the corresponding Si 2p peak area of the respective sample.

reaction (Figure 3a). The presence of a strong C═O stretch vibration at 1715 cm^{-1}, a C−O−H in-plane vibration (1414 cm^{-1}), and the lack of observable Si−O−Si or Si−O−C vibrations (1000−1250 cm^{-1}) provided additional evidence of attachment by the C═C end of the reagent, with the carboxylic acid sites facing out from the Si surface.[30,31] Based on a comparison of the original Si−H FTIR peak area with the decrease in signal observed following hydrosilylation (additional details in the Methods section), the coverage of Si−undecanoic acid surfaces after 5 h (not shown) was estimated to be 44%, assuming initial 100% coverage of Si−H sites on Si(111) surfaces.[33] Unreacted Si−H bonds were confirmed to comprise the remainder of the Si atop site termination.

Figure 2b shows the N 1s region XPS data obtained for Si(111) surfaces functionalized using Boc-aminobutene. Based on the intensity of the NH_2 peak at 400.3 eV, significant attachment was observed after 5 h of reaction time.[34] The coverage under these

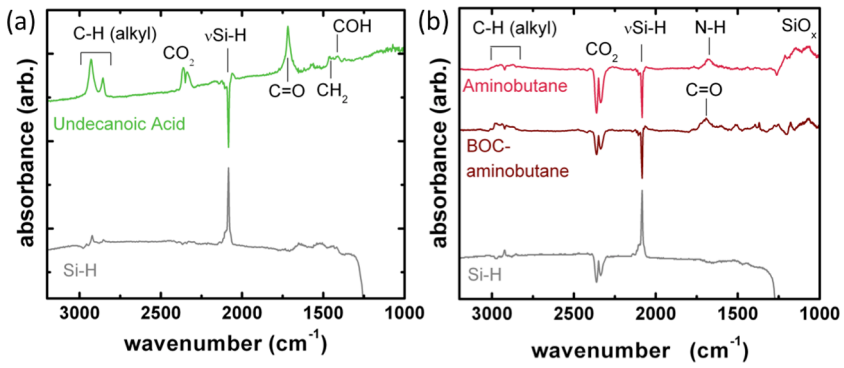

Figure 3. Transmission FTIR spectra of functionalized Si(111) surfaces with (a) Si—undecanoic acid, 3 h reaction time, and (b) Boc-aminobutane, 5 h reaction time followed by subsequent deprotection in TFA ("aminobutane"). In both cases, the spectra for the functionalized surface were measured with respect to the original Si—H background prior to functionalization, shown in gray for each sample.

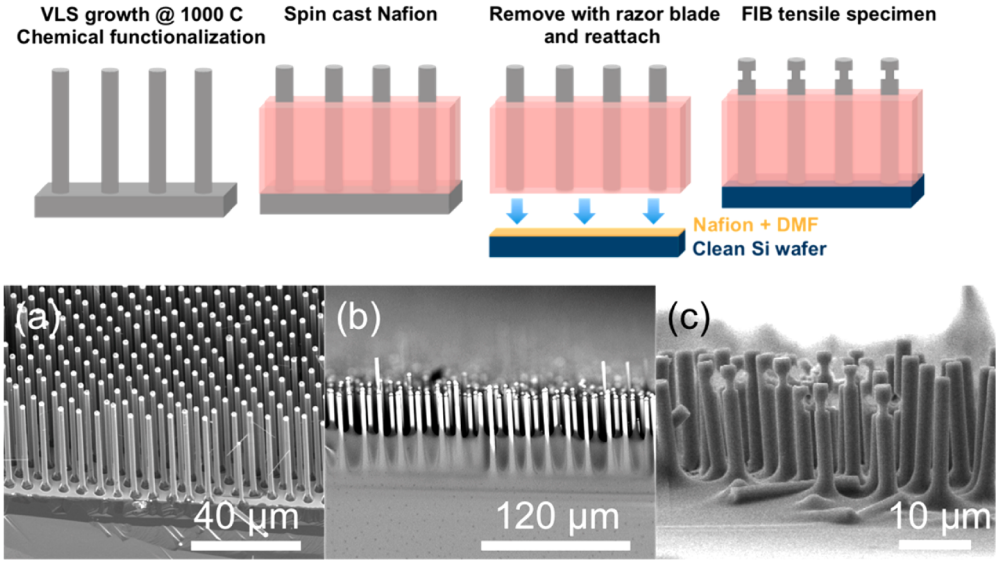

Figure 4. Preparation of samples for mechanical testing. (a) Wire arrays were grown using vapor—liquid—solid growth at 1000 °C, which resulted in high fidelity, vertically aligned wires with ~15—40 μm height. (b) Arrays were embedded in Nafion by spin-casting and were cured and subsequently peeled with a razor blade to detach wires from the growth substrate. (c) FIB milling was used to cut "dog bone" tensile grips into the tops of exposed wires.

conditions, as determined from transmission FTIR (Figure 3), was also 45%, similar to that of Si—undecanoic acid surfaces. Upon deprotection with trifluoroacetic acid (TFA), the intensity of the original NH_2 peak in Figure 2b decreased moderately, presumably due to removal of adsorbed, unreacted molecular layers. A peak was also detected at 402.0 eV, consistent with expectations for NH_3^+ groups[34] that are locally protonated by adsorbed water at the highly basic NH_2 sites. The deprotection of the Boc groups was further supported by a decrease in the magnitude of the absorption peak at 1710 cm^{-1} in the FTIR spectrum attributable to the C═O stretch in the protecting group, the concurrent increase of intensity at 1680 cm^{-1} corresponding to the N—H stretching mode, and a decrease in fingerprint N—C stretches in the 1000—1500 cm^{-1} region (Figure 3 and Supporting Information Figure S3).[35] No SiO_x or Si—N signals were observed in the Si 2p spectrum upon initial functionalization for up to 5 h. However, the deprotection step, which was conducted in air, caused a slight increase in the SiO_x signal (Figure S4), consistent with the oxidation of underlying, nonreacted Si—H sites. Si—CH_3 wire surface terminations, obtained using a sequential chlorination—alkylation Grignard reaction procedure,[36] have been described in detail elsewhere and were directly used in this work without additional spectroscopic characterization.[25]

Si microwire arrays were functionalized *via* as-described hydrosilylation or Grignard reactions immediately prior to bonding with Nafion. In addition to Si—undecanoic acid, Si—aminobutane, and Si—CH_3 surfaces, Si—H and native SiO_x-terminated wires were also prepared. Freshly functionalized arrays were rapidly embedded in Nafion *via* spin-casting of Nafion solutions (27 wt % in dimethylformamide (DMF)) (Figure 4), and the polymer was cured at 120 °C following removal of the solvent by vacuum. A low spin

rate (500 rpm) was necessary during spin-casting to ensure a partial infill of the viscous polymer solution into the array, with higher spin rates resulting in thin (<5 μm) polymer layers that did not provide sufficient mechanical rigidity to maintain microwire alignment throughout subsequent processing steps. The resulting composites consisted of a Nafion layer constrained to a layer at the bottom of the array with ~50% of the wire height embedded, as shown in Figure 4b.

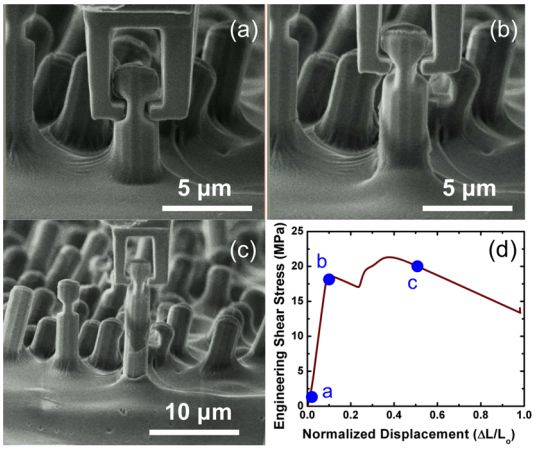

Figure 5. Sequential series of images from the *in situ* SEM observation of a single-wire pull-out test (Si−aminobutane, 3 h). (a) Placement of the grips around the sample prior to loading; (b) initial elastic loading of the polymer; (c) sliding of the debonded wire out of the Nafion matrix; and (d) engineering shear stress *vs* normalized displacement. Data points (blue dots) correspond to images (a−c).

Interestingly, the Nafion film exhibited an upward rise in the vicinity of the wire that occurred regardless of surface chemistry (Figure S5) and that did not correlate with the resulting mechanical adhesion (*vide infra*). This rise is therefore believed to be representative of the flow properties of the viscous Nafion solution under relatively slow spinning conditions, in combination with the rapid curing process, rather than of the wetting behavior of Nafion with different surface chemistries. The polymer-embedded array was subsequently detached from the growth substrate along the base using a razor blade. The wires were glued with a thin layer of Nafion−DMF to a clean Si substrate and cured, which led to all of the bonding wire surfaces (including the bottom surface of the wire) being embedded in Nafion. To prepare the individual wires for nanomechanical pull-out experiments, the "heads" of the Si microwires were carved into dog-bone-like shapes by a focused ion beam (FIB) to conform to the diamond grips that were used for the nanomechanical measurements (Figures 4c and 5).

The mechanical response revealed several distinct regimes of behavior (Figure 5), which were qualitatively similar among all examined surfaces (Figure 6). The initial, linear relationship between the applied load and displacement as well as observations in the corresponding SEM images (Figure 5) indicated that the Nafion in the vicinity of the wire was elastically stretched with no relative sliding at the Si microwire−polymer interface. The point of maximum load occurred when the wire first debonded from the polymer and began to

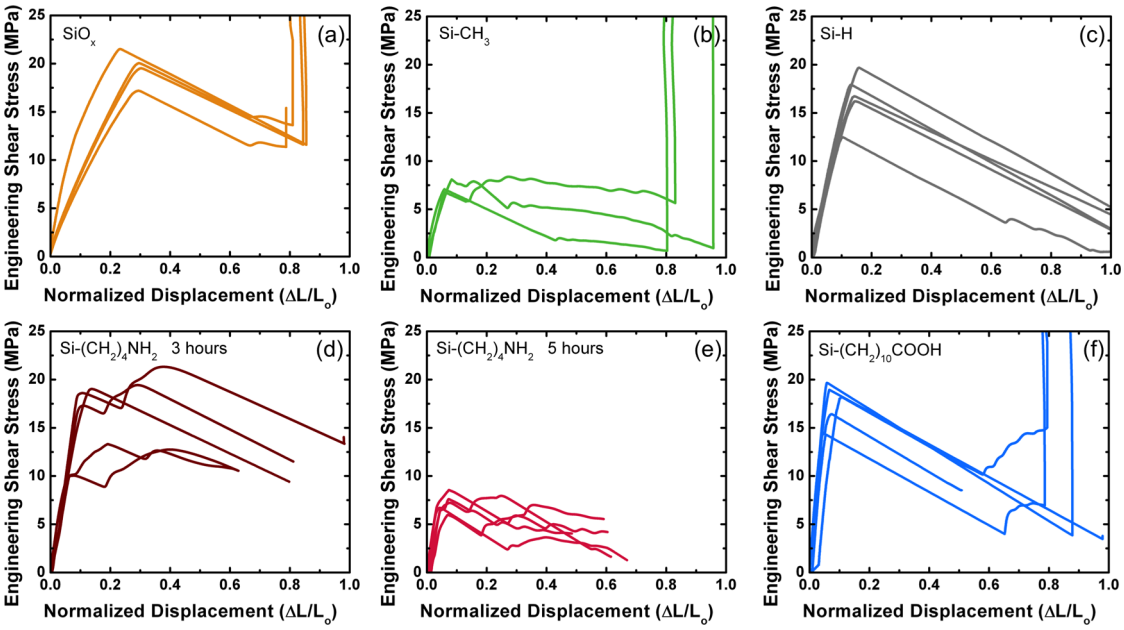

Figure 6. Stress *vs* strain for nanomechanical pull-out experiments on individual Si microwires functionalized with (a) native oxide (SiO_x), (b) methyl ($Si-CH_3$), (c) hydride (Si−H), (d) aminobutane ($Si-(CH_2)_4NH_2$) for 3 h, (e) aminobutane for 5 h, and (f) undecanoic acid ($Si-(CH_2)_{10}COOH$) surfaces. The engineering shear stress was obtained by dividing the measured load in millinewtons by the initial embedded contact area of the wire, while the normalized displacement was computed by dividing the change in length, ΔL, by the initial embedded wire length, L_0. In (d,e), the onset of debonding occurred upon reaching the first stress maximum, as observed in the SEM during the measurements.

slide out, with some friction, from the matrix while the polymer around the wire relaxed to its unloaded state. In the process of extracting the wire, the contact area between the wire and the polymer decreased, which lowered the amount of friction between the wire and polymer and thus decreased the applied load necessary to overcome this friction. The surfaces of the wires after extraction were physically equivalent to those in the as-grown state and were covered with no polymer debris, as evidenced by the observation of crystallographic facets for all surface terminations. This characteristic allowed for relatively accurate measurements of the wire dimensions (Figure S6).

The maximum engineering shear stress, which was computed based on the measured maximum load in millinewtons (F_{max}) and the embedded wire dimensions before debonding (average diameter, d_{avg}, and original length, L_0) as $\sigma_{max} = F_{max}/\pi d_{avg} L_0$, had a clear dependence on the surface chemistry (Figure 6). The highest maximum shear stress, 19.8 ± 1.7 MPa, was observed for SiO_x-terminated Si microwires (Figure 6a). A significantly lower maximum shear stress, 7.3 ± 0.6 MPa, was observed for the CH_3-terminated Si microwires (Figure 6b). For comparison, the shear strength of H-terminated Si microwires was 16.5 ± 3.3 MPa (Figure 6c) and was thus comparable to that of SiO_x-terminated wires, within the measurement uncertainty. These results were self-consistent and reproducible across all of the wires in different regions of the sample.

Aminobutane-terminated Si microwire surfaces were prepared with two functionalization times, 3 and 5 h, to investigate the influence of reaction time and surface coverage on the maximum interfacial shear stress (Figure 6d,e). The microwires that had been functionalized for a 3 h reaction time exhibited an average maximum shear stress of 15.7 ± 3.8 MPa, statistically similar to that of SiO_x- and H-terminated Si microwires. The maximum average shear stress in samples reacted for 5 h was a factor of 2 lower, at 7.2 ± 1.0 MPa, which could be caused by the evolution in surface coverage and structure of hydrosilylated surfaces with time. Water contact-angle measurements (Figure S7) as a function of reaction time for amine-functionalized surfaces showed a concurrent significant change from a hydrophobic (~90°) contact angle for 1 and 3 h reaction times to a more hydrophilic surface (61 ± 2°) after a 5 h reaction time. The average maximum shear stress for undecanoic acid-terminated Si microwire surfaces (Figure 6f) was 16.3 ± 1.9 MPa, which is similar to that of the SiO_x-terminated surfaces. Figure 7 presents a comparison of the maximum shear stress for all of the surface chemistries investigated herein.

The decreasing effective embedded length of each post-debonded wire enabled the calculation of a true shear stress, defined as the applied force divided by the instantaneous interfacial contact area.

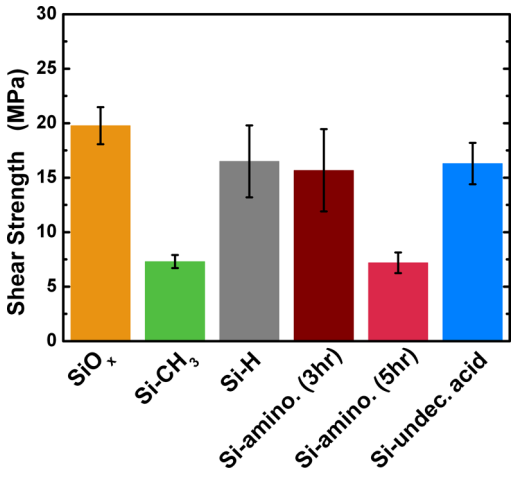

Figure 7. Comparison of interfacial shear strengths obtained from the data shown in Figure 6.

Figure S8 presents the true stress of a representative wire chosen from each surface chemistry. In all cases, the true stress remained virtually constant after delamination during the dissipative shearing from the Nafion matrix. This behavior suggests that molecular bonds provide the primary factor that determines the adhesion between the Si and the polymer matrix because the interactions per unit contact area did not vary as a function of the total embedded length.

The maximum shear stresses (Figure 8a) and adhesion energies (Figure 8b) obtained from the pull-out experiments can be compared to selected micro- and nanoscale measurements of intermolecular adhesive forces reported previously,[12,14,25,37,38] as well as to the values reported for macroscale laminate, adhesive, and polymer coatings.[9,39,40] The 7−20 MPa interfacial shear stresses observed between the Si microwires and Nafion are comparable to the grafting stresses reported between carbon nanotube (CNT) and carbon nanofiber interfaces of ~5−25 MPa[38] adhered by van der Waals interactions and are higher than the shear stresses reported for CNT/SiC[37] (~0.5 MPa) and in polyethylene terephthalate (PET)/silicone[9] (0.5−4.5 MPa) systems. The maximum shear stresses measured herein were also up to a factor of 2.5 higher than those observed previously for similarly functionalized Si microwires embedded in a polydimethylsiloxane (PDMS) matrix and determined using the same mechanical testing methodology.[25] The interfacial adhesion energy (Figure 8b), which ranged from 1−13 J m^{-2}, also agreed well with reported adhesion energies in literature, including PMMA/adhesive,[14] Si/polystyrene,[12] Si/Si wafer bonded,[41] and SiN_x/organosilicate adhesive[39] interfaces. A critical value of 5 J m^{-2} is often cited as an industry standard for the minimal adhesive energy required for robust laminates and coatings for practical applications.[42] In several of the surfaces (Si−undecanoic, SiO_x, and Si−H) tested in this work, this value was exceeded by more than a factor of 2.

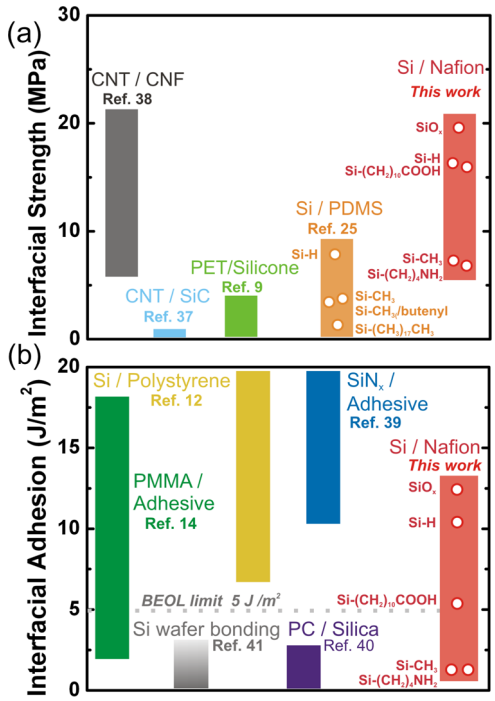

Figure 8. Comparison of ranges of interfacial strength and adhesion obtained in this study with reported literature values. (a) Shear stress resulting from bonding of Si microwires in Nafion and PDMS obtained from *in situ* wire pull-out tests and of bonding between PET/silicone laminates,[9] CNT bristles on SiC,[37] and CNTs grown on carbon nanofibers.[38] The shear strength data reported in literature were obtained using a range of mechanical testing methodologies. (b) Comparison of interfacial adhesion in J m^{-2} of Si microwires in Nafion with literature values obtained from peel or fracture tests of a range of interfaces: SiN_x/adhesive,[39] PC/silica,[40] Si/polystyrene,[12] and PMMA/adhesive,[14] as well as Si wafer bonding.[41] The BEOL industrial target[42] of 5 J m^{-2} for strong coating adhesion is indicated (dashed line). Bars represent a range of reported values for various interfaces.

DISCUSSION

The regeneration of the smooth facets on the Si wire surfaces in the postextraction samples indicates that the interface between the Nafion matrix and the Si was the weakest link in the composite system. The molecular surface that formed as a result of chemical functionalization drove the initial adhesion between the Nafion and the wire surfaces, and the resulting molecular layer/Nafion bonds were fully severed upon extraction of the wire. This behavior strongly suggests that the *in situ* mechanical experiments measured the bond strength and failure within the molecular interface layer, rather than fracture within the Nafion membrane or elsewhere within the composite. A reasonable interpretation of the data is that the maximum shear stress determined herein therefore provides a measure of the bond strength of functionalized Si wires arising from different chemical interactions.

The relatively high shear strength of ~16–20 MPa exhibited by the SiO_x and oxygen-containing Si microwire surfaces agrees well with general surface adhesion methodologies reported previously, in which oxidized Si surfaces are commonly promoted by oxygen plasma[14] or chemical treatments to take advantage of polar interactions with polymers. In the experiments described herein, hydroxylated[43,44] SiO_x surfaces can participate in bonding with Nafion *via* hydrogen bonding, whose energy is on the order of 10–40 kJ mol,[23] with oxygen in the hydrophilic side chains within the Nafion structure. The lower shear strength of 7.3 ± 0.6 MPa observed for the Si–CH_3-functionalized Si microwires is also reasonable given the inert and hydrophobic nature of Si–CH_3 surfaces. CH_3-terminated Si microwires are expected to interact primarily with the PTFE Nafion backbone *via* weak van der Waals forces, whose energies have been reported to be 0.1–10 kJ mol^{-1},[23] which are in accord with the approximately 3-fold lower interfacial shear strength observed relative to the sheer strength for the SiO_x-terminated microwires. This finding of low shear strength for the methyl-terminated Si wires agrees well with earlier findings of the relatively low interfacial adhesion of 4.1 MPa attained with Si–CH_3 wires in a PDMS matrix.[25]

Si–H surfaces are typically hydrophobic, and it would be reasonable to hypothesize that such surfaces would experience weak van der Waals interactions with the hydrophobic Nafion backbone, similar to those for Si–CH_3 surfaces. However, the high shear strength measured herein for the Si–H-terminated wires indicates that a different chemical interaction occurs in practice. The similarity between the Si–H and SiO_x shear strengths is consistent with oxidation of the Si–H-functionalized surfaces in the presence of the polymer solution (Nafion in DMF) during spin-casting and curing in ambient conditions, which instead could promote chemical interaction *via* hydrogen bonding with acidic groups in Nafion side chains. An increase in shear strength was observed previously with PDMS for Si–H-terminated surfaces as compared to Si–CH_3-terminated surfaces.[25] This behavior was attributed to the presence of a competitive hydrosilylation reaction between Si–H and olefin terminal groups in the PDMS prepolymer solution, the rapid kinetics of which "quenched" the Si–H groups before oxidation could occur. In the absence of such a competitive reaction, Si–H can rapidly convert to Si–OH or to other oxidized groups, which would then govern the interfacial adhesion. This finding has practical significance for surfaces terminated herein with alkanes *via* hydrosilyation, as approximately 50% of the surface bonds are unreacted as Si–H.

The greater than 2-fold reduction in shear strength with increasing reaction time observed for the Si–aminobutane surfaces reveals that the molecular surface structure can play an important role in determining the mechanical properties of the composite. With shorter reaction times, a higher population of surface moieties remain as unreacted Si–H sites,

as evidenced from FTIR measurements (Figure S9). These sites can then oxidize and promote strong interfacial adhesion, as was observed for the Si−H- and SiO_x-terminated Si microwires. With longer reaction times, the wire surfaces became saturated at 45% coverage of aminobutane, so for such samples, the mechanical properties are increasingly governed by the amine−Nafion (7.2 ± 1.0 MPa) interaction as compared to the interaction between the Nafion and the underlying SiO_x. This change in surface functionality is supported by water contact-angle measurements (Figure S7) on a partially amine-functionalized Si(111) surface, which showed a significant change from a hydrophobic (90 ± 2°) contact angle for 1 and 3 h reaction times to a more hydrophilic surface (61 ± 2°) after a 5 h reaction time, presumably resulting from an increase in the coverage of the hydrophilic amine termination groups. Although Si−H microwires become oxidized during Nafion spin-casting and subsequent processing for mechanical tests, the Si−H planar surfaces used for the contact-angle measurements likely remained stable with Si−H surface termination over the short time scales of the contact-angle measurements, and the contact-angle data thus served as an indication of the relative predominance of unreacted Si−H sites rather than an indication of the interaction strength with Nafion. Consistently, after 90 h of exposure to ambient air, the contact angle of the Si−H-functionalized surface decreased from 87 ± 1 to 72 ± 3°, presumably resulting from the gradual oxidation of Si−H surface sites producing an increase in surface hydrophilicity. The contact angle of the air-exposed, partially oxidized Si−H surface was comparable to that of a Si−undecanoic acid surface (73 ± 2°, 5 h reaction time, Figure S7), in accord with the comparable shear strengths measured for these two surfaces.

The significant decrease in maximum shear stress between 3 and 5 h amine surfaces reveals the effects associated with chemical interactions between the amine moieties and the Nafion. The highly basic amine sites might be expected to function as target proton acceptors from $-SO_3H$ groups in the Nafion side chains, giving rise to electrostatic interactions between NH_3^+ and SO_3^-, which would be expected to be relatively strong. However, the data suggest that the surfaces of amine-terminated wires can be complex. Indeed, the spectroscopic data revealed several populations of surface species following deprotection in TFA, including amine (NH_2), ammonium (NH_3^+, Figure 2b), and unreacted Si−H groups (Figure 3). Although $-NH_2$ groups can participate in hydrogen bonding with the Nafion side chains as well as participate in possible electrostatic reactions, the protonation to NH_3^+, which occurs readily in ambient due to the high pK_a of ∼10 for aliphatic amines,[45] can screen interactions with terminal $-SO_3H$ groups. The mechanical response probes an average of these interactions, which could plausibly then result in a weaker overall observed mechanical shear strength. We note that the hydrophilicity of Si−amine (5 h) samples observed from contact-angle measurements (Figure S7) only indicates the presence of polar groups on the surface but cannot distinguish between NH_2 or protonated NH_3^+ surfaces and thus does not predict strong interactions based on hydrophilic arguments alone.

The similarity between the mechanical shear strengths in the undecanoic acid, SiO_x, and oxidized Si−H microwire surfaces indicates that oxygen-containing groups are important for tailoring strong interfacial adhesion in ionomers with hydrophilic constituents. However, SiO_x surfaces and air-exposed Si−H surfaces are known to exhibit high surface-recombination velocities,[16] indicative of the presence of surface defects which act as trap states[46] and which result in poor electronic quality of these surfaces for photoelectrochemical and electronic applications. Therefore, compared to native SiO_x, the undecanoic acid surfaces provide an advantage by shifting the bonding plane away from the Si surface, allowing for oxygen−Nafion bonding while minimizing formation of deleterious Si−O bonds. Although the hydrosilylation reactions employed herein can leave up to ∼50% of surface sites remaining as Si−H, our spectroscopic evidence reveals minimal SiO_x formation, possibly due to the blocking structure of the bulky overlayers and subsequent protection of remaining Si−H sites against air reactivity. Our results indicate that further efforts to develop reaction schemes that maximally passivate the unreacted Si−H sites left by hydrosilylation represent a promising strategy to tailor surfaces to obtain combined electronic and mechanical performance.

The mechanical response of functionalized Si microwires following the initial debonding event revealed qualitative evidence that the wire surfaces continuously interacted with the Nafion as the wire was slowly removed from the polymer. This behavior was evidenced by the nearly constant observed true stress, which was independent of the length of the embedded wire (Figure S8). For the functionalizations that resulted in weaker interactions, such as Si−CH_3 and Si−aminobutane, weak oscillations were observed in the measured force and computed engineering and true stresses (Figures 6 and S8), but these oscillations were not observed for systems having stronger interactions. The oscillations could result from the inherently weaker intermolecular forces involved in bonding to Nafion for these particular chemistries, which would permit a greater slipping and relaxation of applied load before the bonds could re-form at the sliding interface. The physical origin of these oscillations, which may be strain-rate-dependent, represents a focus for future work. The results of this study reveal

that nanoscale mechanical testing can reveal rich information on molecular-scale interactions and that such chemical functionalization can be suitable for use in real devices.

CONCLUSIONS

In situ nanomechanical testing has provided insight regarding the chemical origin of the interfacial shear strength in a functionalized Si microwire−Nafion composite. A range of surface functionalities, chain lengths, and coverages were chosen to target interactions with different regions of the Nafion chains. The interaction strength was reduced for longer functionalization durations of an aminobutene molecular layer, from 15.7 ± 3.8 MPa for 3 h reaction time to 7.2 ± 1.0 MPa for 5 h long reactions. This behavior suggests that increasing coverage of the surface layer can push the bonding plane away from the underlying SiO_x surface. Additionally, the interfacial shear strength can be increased at similar coverages (~50%) by functionalizing the Si surface with carbonyl or hydroxyl moieties, which promotes strong bonding to hydrophilic side chains in Nafion (*e.g.*, 16.3 ± 1.9 MPa for a Si−undecanoic acid surface). The methodology for such chemical−nanomechanical experiments, which utilizes a well-defined interfacial geometry, simple loading conditions, and the ability to measure mechanical stresses and strains of functionalized Si surfaces, is a generalizable platform for quantifying the molecular origin of mechanical behavior.

METHODS

Wire Growth. Intrinsic Si wire arrays were grown using a vapor−liquid−solid chemical vapor deposition process with H_2 and $SiCl_4$ as reactants and a photolithographically patterned Cu catalyst, as reported previously.[25,47] Growth was performed at 1000 °C, and the wire height, which was controlled by modulating the growth time, typically ranged between 15 and 40 μm with wire diameters of approximately 1.5−2.0 μm. Following growth, arrays were etched in buffered HF (Transene Co.) for 30 s, rinsed copiously with water, and submerged in an RCA II (5:1:1 $H_2O/HCl/H_2O_2$) etch for 25 min to dissolve the Cu catalyst. The resulting arrays were rinsed with deionized H_2O and dried under N_2(g).

Surface Functionalization. Wires with a native oxide (SiO_x) fully enveloping the surface were obtained by leaving as-prepared samples in ambient air for several days. Si−H wires were obtained by immersing RCA-cleaned arrays into buffered HF(aq) for 30 s, followed by thorough rinsing with water and drying under N_2(g). Si−CH_3 wires were prepared using a chlorination−alkylation Grignard process adapted for Si microwire arrays, as reported in detail previously.[25] Hydrosilylation reactions were conducted on freshly H-terminated wires that were transferred immediately to a N_2(g)-purged flushbox to minimize exposure to air. Samples were contained in a sealed-bottom quartz tube in the reaction solution and were irradiated for the desired reaction time with short-wave (254 nm) UV light from below the sample. Si−undecanoic acid (Si−$(CH_2)_{10}$COOH) surfaces were obtained in this manner by using 10% (by volume) undecylenic acid (Sigma-Aldrich, ≥95%) in low-water toluene (JT Baker). The surfaces were then rinsed in hot (90 °C) acetic acid for 5 min.[30] Amine-terminated Si microwires were obtained similarly using 10% (by volume) 1-(Boc-amino)-3-butene (Sigma-Aldrich, 97%) in toluene. Functionalized planar Si(111) surfaces (Addison Engineering, Inc., n-type (phosphorus-doped), double-side polished, 500 ± 20 μm, >20 000 Ω·cm) were cleaned prior to surface analysis by sonication for 1−3 min in toluene. Si microwires were rinsed by immersion in toluene in a test tube, followed by manual agitation for 1 min. Following functionalization and cleaning, the Boc protecting group of the aminobutane surface was removed in air by soaking the sample for 1 h in a 1:2 (v/v) solution of trifluoroacetic acid in dichloromethane.

Surface Characterization. XPS data were collected using a Surface Science Instruments M-Probe ESCA controlled by Hawk Data Collection software. The X-ray source was a monochromatic Al Kα line at 1486.6 eV. High-resolution scan intensities were normalized to the Si 2p peak area for comparison across samples. Transmission FTIR data were collected in dry N_2(g) using a Nicolet 6700 spectrometer with a 4 cm^{-1} resolution. Spectra of Si−H wafers were referenced to their original SiO_x spectra (prior to etching), and hydrosilylated surfaces were referenced to the Si−H spectra of the same wafers (prior to UV reaction). The molecular coverage of these surfaces was then estimated from the ratio of the decrease in Si−H stretch at 2081 cm^{-1} after hydrosilylation to the original area of the Si−H stretch on the same surface. Assuming 100% coverage of Si(111)−H sites prior to hydrosilylation,[33] the surface coverage percentage was directly estimated from this ratio.

Sample Preparation. The perfluorosulfonic acid−PTFE copolymer (Nafion) solution was prepared *via* solvent exchange by slowly evaporating an aqueous Nafion solution (0.9 mequiv g^{-1} exchange capacity, 5% w/w in a water/alcohol mixture, Alfa Aesar) in DMF until all water was removed to yield a 27% (by weight) solution. Functionalized Si microwire arrays were embedded in Nafion by spin-casting (400 rpm, 30 s). The arrays were then placed in a vacuum oven at room temperature to evaporate the solvent and were cured at 120 °C on a hot plate in air for at least 20 min. Following curing, the embedded arrays were removed from the substrate by slicing along the polymer−Si substrate interface with a razor blade (Figure 4), similar to the nanomechanical wire pull-out sample-preparation procedure that has been reported previously.[25] The freestanding array was then transferred to a clean Si substrate and was re-adhered by spinning a thin layer (1000 rpm) of the same Nafion−DMF solution. The DMF acted as "glue" by dissolving the very bottom layer of the polymer and anchoring it to the underlying Si substrate. The thin adhesive layer was then dried and cured in the same manner as the bulk Nafion film. This transfer procedure left the tops of the wires exposed. "Dog bone" shapes were carved into individual wires using a focused ion beam (Versa 3D DualBeam, FEI).

***In Situ* Nanomechanical Experiments.** Uniaxial pull-out tests were performed in a custom-made *in situ* nanomechanical instrument, named the SEMentor, in a similar procedure to that developed by Cho *et al.*[25] A constant displacement rate of 50 nm s^{-1} was prescribed, and load and displacement data were then obtained. Upon completion of the experiment, which corresponded to the complete detachment of the microwire from the matrix, the initial embedded wire length and the average wire diameter were measured in the SEM, which enabled the estimation of the embedded surface area under the assumption of a cylindrical cross section, $\pi d_{avg} L_0$. The engineering shear stress was calculated by dividing the applied load by the embedded surface area, and the true shear stress during the wire removal phase was computed by normalizing to the instantaneous contacting surface area, $A_{true} = \pi d_{avg}(L_0 - rt)$, where r is the known displacement rate. Then, 3−5 pull-out tests were conducted for each wire array (one array per surface chemistry) to ensure reproducibility. The adhesion energy was estimated by the relationship $E = 1/2 F_{max} \Delta L$, where ΔL is the wire-polymer displacement at the instance of debonding, under the assumption that all of the elastic strain energy that

accumulated within the polymer at debonding was transferred directly into the newly formed surface energy caused by debonding. This assumption is reasonable because debonding was found to occur within the elastic loading region of the polymer without observation in the mechanical data of plastic dissipation and because the lack of relative motion at the wire–Nafion interface at the instance of debonding suggested minimal dissipation of stored energy into friction.

Conflict of Interest: The authors declare no competing financial interest.

Acknowledgment. This research made use of the Shared Experimental Facilities supported by the Molecular Materials Research Center at the California Institute of Technology and of funds provided by the National Science Foundation (NSF) Center for Chemical Innovation: Solar Fuels (Grant CHE-1305124). B.M.G. acknowledges financial support from a Caltech Kavli Nanoscience Institute Prize Postdoctoral Fellowship.

Supporting Information Available: Additional XPS and FTIR data, SEM images from mechanical testing, true stress *vs* strain data, water contact-angle measurements. This material is available free of charge *via* the Internet at http://pubs.acs.org.

REFERENCES AND NOTES

1. Rogers, J. A.; Someya, T.; Huang, Y. G. Materials and Mechanics for Stretchable Electronics. *Science* **2010**, *327*, 1603–1607.
2. McAlpine, M. C.; Ahmad, H.; Wang, D. W.; Heath, J. R. Highly Ordered Nanowire Arrays on Plastic Substrates for Ultrasensitive Flexible Chemical Sensors. *Nat. Mater.* **2007**, *6*, 379–384.
3. Nadarajah, A.; Word, R. C.; Meiss, J.; Konenkamp, R. Flexible Inorganic Nanowire Light-Emitting Diode. *Nano Lett.* **2008**, *8*, 534–537.
4. Zhang, B. W.; Dong, Q.; Korman, C. E.; Li, Z. Y.; Zaghloul, M. E. Flexible Packaging of Solid-State Integrated Circuit Chips with Elastomeric Microfluidics. *Sci. Rep.* **2013**, *3*, 1–8.
5. Carli, S.; Casarin, L.; Bergamini, G.; Caramori, S.; Bignozzi, C. A. Conductive PEDOT Covalently Bound to Transparent FTO Electrodes. *J. Phys. Chem. C* **2014**, *118*, 16782–16790.
6. Fan, Z. Y.; Razavi, H.; Do, J. W.; Moriwaki, A.; Ergen, O.; Chueh, Y. L.; Leu, P. W.; Ho, J. C.; Takahashi, T.; Reichertz, L. A.; et al. Three-Dimensional Nanopillar-Array Photovoltaics on Low-Cost and Flexible Substrates. *Nat. Mater.* **2009**, *8*, 648–653.
7. Walter, M. G.; Warren, E. L.; McKone, J. R.; Boettcher, S. W.; Mi, Q. X.; Santori, E. A.; Lewis, N. S. Solar Water Splitting Cells. *Chem. Rev.* **2010**, *110*, 6446–6473.
8. Warren, E. L.; Atwater, H. A.; Lewis, N. S. Silicon Microwire Arrays for Solar Energy-Conversion Applications. *J. Phys. Chem. C* **2014**, *118*, 747–759.
9. Zhang, C.; Shephard, N. E.; Rhodes, S. M.; Chen, Z. Headgroup Effect on Silane Structures at Buried Polymer/Silane and Polymer/Polymer Interfaces and Their Relations to Adhesion. *Langmuir* **2012**, *28*, 6052–6059.
10. Lesho, M. J.; Sheppard, N. F. Adhesion of Polymer Films to Oxidized Silicon and Its Effect on Performance of a Conductometric pH Sensor. *Sens. Actuators, B* **1996**, *37*, 61–66.
11. Bhairamadgi, N. S.; Pujari, S. P.; Leermakers, F. A. M.; van Rijn, C. J. M; Zuilhof, H. Adhesion and Friction Properties of Polymer Brushes: Fluoro *versus* Nonfluoro Polymer Brushes at Varying Thickness. *Langmuir* **2014**, *30*, 2068–2076.
12. Vyas, M. K.; Schneider, K.; Nandan, B.; Stamm, M. Switching of Friction by Binary Polymer Brushes. *Soft Matter* **2008**, *4*, 1024–1032.
13. Uddin, M. A.; Ho, W. F.; Chow, C. K.; Chan, H. P. Interfacial Adhesion of Spin-Coated Thin Adhesive Film on Silicon Substrate for the Fabrication of Polymer Optical Waveguide. *J. Electron. Mater.* **2006**, *35*, 1558–1565.
14. Cui, L. Y.; Lionti, K.; Ranade, A.; Larson-Smith, K.; Dubois, G. J. M.; Dauskardt, R. H. Highly Transparent Multifunctional Bilayer Coatings on Polymers Using Low-Temperature Atmospheric Plasma Deposition. *ACS Nano* **2014**, *8*, 7186–7191.
15. Lee, K. J.; Tosser, K. A.; Nuzzo, R. G. Fabrication of Stable Metallic Patterns Embedded in Poly(dimethylsiloxane) and Model Applications in Non-planar Electronic and Lab-on-a-Chip Device Patterning. *Adv. Funct. Mater.* **2005**, *15*, 557–566.
16. Royea, W. J.; Juang, A.; Lewis, N. S. Preparation of Air-Stable, Low Recombination Velocity Si(111) Surfaces through Alkyl Termination. *Appl. Phys. Lett.* **2000**, *77*, 1988–1990.
17. McFarlane, S. L.; Day, B. A.; McEleney, K.; Freund, M. S.; Lewis, N. S. Designing Electronic/Ionic Conducting Membranes for Artificial Photosynthesis. *Energy Environ. Sci.* **2011**, *4*, 1700–1703.
18. Plass, K. E.; Filler, M. A.; Spurgeon, J. M.; Kayes, B. M.; Maldonado, S.; Brunschwig, B. S.; Atwater, H. A.; Lewis, N. S. Flexible Polymer-Embedded Si Wire Arrays. *Adv. Mater.* **2009**, *21*, 325–328.
19. Spurgeon, J. M.; Walter, M. G.; Zhou, J. F.; Kohl, P. A.; Lewis, N. S. Electrical Conductivity, Ionic Conductivity, Optical Absorption, and Gas Separation Properties of Ionically Conductive Polymer Membranes Embedded with Si Microwire Arrays. *Energy Environ. Sci.* **2011**, *4*, 1772–1780.
20. Kreuer, K. D. On the Development of Proton Conducting Polymer Membranes for Hydrogen and Methanol Fuel Cells. *J. Membr. Sci.* **2001**, *185*, 29–39.
21. Mauritz, K. A.; Moore, R. B. State of Understanding of Nafion. *Chem. Rev.* **2004**, *104*, 4535–4585.
22. Ma, C. H.; Yu, T. L.; Lin, H. L.; Huang, Y. T.; Chen, Y. L.; Jeng, U. S.; Lai, Y. H.; Sun, Y. S. Morphology and Properties of Nafion Membranes Prepared by Solution Casting. *Polymer* **2009**, *50*, 1764–1777.
23. Ebbing, D.; Gammon, S. D. *General Chemistry*, 8th ed.; Houghton Mifflin: Boston, MA, 2008.
24. Boyer, R. *Interactive Concepts in Biochemistry*, 2nd ed.; John Wiley & Sons: New York, 2002.
25. Cho, C. J.; O'Leary, L.; Lewis, N. S.; Greer, J. R. *In Situ* Nanomechanical Measurements of Interfacial Strength in Membrane-Embedded Chemically Functionalized Si Microwires for Flexible Solar Cells. *Nano Lett.* **2012**, *12*, 3296–3301.
26. Ciampi, S.; Harper, J. B.; Gooding, J. J. Wet Chemical Routes to the Assembly of Organic Monolayers on Silicon Surfaces *via* the Formation of Si–C Bonds: Surface Preparation, Passivation and Functionalization. *Chem. Soc. Rev.* **2010**, *39*, 2158–2183.
27. Wang, X.; Landis, E. C.; Franking, R.; Hamers, R. J. Surface Chemistry for Stable and Smart Molecular and Biomolecular Interfaces *via* Photochemical Grafting of Alkenes. *Acc. Chem. Res.* **2010**, *43*, 1205–1215.
28. Migas, D. B.; Borisenko, V. E. The Role of Morphology in Stability of Si Nanowires. *J. Appl. Phys.* **2009**, *105*, 104316.
29. Voicu, R.; Boukherroub, R.; Bartzoka, V.; Ward, T.; Wojtyk, J. T. C.; Wayner, D. D. M. Formation, Characterization, and Chemistry of Undecanoic Acid Terminated Silicon Surfaces: Patterning and Immobilization of DNA. *Langmuir* **2004**, *20*, 11713–11720.
30. Faucheux, A.; Gouget-Laemmel, A. C.; de Villeneuve, C. H.; Boukherroub, R.; Ozanam, F.; Allonge, P.; Chazalviel, J.-N. Well-Defined Carboxyl-Terminated Alkyl Monolayers Grafted onto H-Si(111): Packing Density from a Combined AFM and Quantitative IR Study. *Langmuir* **2006**, *22*, 153–162.
31. Asanuma, H.; Lopinski, G. P.; Yu, H.-Z. Kinetic Control of the Photochemical Reactivity of Hydrogen-Terminated Silicon with Bifunctional Molecules. *Langmuir* **2005**, *21*, 5013–5018.
32. Strother, T.; Cai, W.; Zhao, X.; Hamers, R. J.; Smith, L. M. Synthesis and Characterization of DNA-Modified Silicon (111) Surfaces. *J. Am. Chem. Soc.* **2000**, *122*, 1205–1209.
33. Higashi, G. S.; Chabal, Y. J.; Trucks, G. W.; Raghavachari, K. Ideal Hydrogen Termination of the Si-(111) Surface. *Appl. Phys. Lett.* **1990**, *56*, 656–658.

34. Strother, T.; Hamers, R. J.; Smith, L. M. Covalent Attachment of Oligodeoxyribonucleotides to Amine-Modified Si(001) Surfaces. *Nucleic Acids Res.* **2000**, *8*, 3535–3541.
35. Maier, A.; Tieke, B. Coordinative Layer-by-Layer Assembly of Electrochromic Thin Films Based on Metal Ion Complexes of Terpyridine-Substituted Polyaniline Derivatives. *J. Phys. Chem. B* **2012**, *116*, 925–934.
36. Bansal, A.; Li, X. L.; Lauermann, I.; Lewis, N. S.; Yi, S. I.; Weinberg, W. H. Alkylation of Si Surfaces Using a Two-Step Halogenation Grignard Route. *J. Am. Chem. Soc.* **1996**, *118*, 7225–7226.
37. Cao, A. Y.; Veedu, V. P.; Li, X. S.; Yao, Z. L.; Ghasemi-Nejhad, M. N.; Ajayan, P. M. Multifunctional Brushes Made from Carbon Nanotubes. *Nat. Mater.* **2005**, *4*, 540–545.
38. He, X. D.; Wang, C.; Tong, L. Y.; Wang, R. G.; Cao, A. Y.; Peng, Q. Y.; Moody, S.; Li, Y. B. Direct Measurement of Grafting Strength between an Individual Carbon Nanotube and a Carbon Fiber. *Carbon* **2012**, *50*, 3782–3788.
39. Hohlfelder, R. J.; Maidenberg, D. A.; Dauskardt, R. H.; Wei, Y. G.; Hutchinson, J. W. Adhesion of Benzocyclobutene-Passivated Silicon in Epoxy Layered Structures. *J. Mater. Res.* **2001**, *16*, 243–255.
40. Lionti, K.; Cui, L. Y.; Volksen, W.; Dauskardt, R.; Dubois, G.; Toury, B. Independent Control of Adhesive and Bulk Properties of Hybrid Silica Coatings on Polycarbonate. *ACS Appl. Mater. Interfaces* **2013**, *5*, 11276–11280.
41. Gosele, U.; Stenzel, H.; Martini, T.; Steinkirchner, J.; Conrad, D.; Scheerschmidt, K. Self-Propagating Room-Temperature Silicon-Wafer Bonding in Ultrahigh-Vacuum. *Appl. Phys. Lett.* **1995**, *67*, 3614–3616.
42. Li, Y. *Microelectronic Applications of Chemical Mechanical Planarization*; John Wiley and Sons: New York, 2007.
43. Nagasawa, Y.; Ishida, H.; Soeda, F.; Ishitani, A.; Yoshii, I.; Yamamoto, K. FTIR-ATR Observation of SiOH and Si-H in the Oxide Layer on an Si Wafer. *Microchim. Acta* **1988**, *1*, 431–434.
44. Theil, J. A.; Tsu, D. V.; Watkins, M. W.; Kim, S. S.; Lucovsky, G. Local Bonding Environments of Si-OH Groups in SiO_2 Deposited by Remote Plasma-Enhanced Chemical Vapor-Deposition and Incorporated by Postdeposition Exposure to Water-Vapor. *J. Vac. Sci. Technol., A* **1990**, *8*, 1374–1381.
45. Graton, J.; Laurence, C.; Berthelot, M.; Le Questel, J. Y.; Besseau, F.; Raczynska, E. D. Hydrogen-Bond Basicity pK_{HB} Scale of Aliphatic Primary Amines. *J. Chem. Soc., Perkin Trans. 2* **1999**, *5*, 997–1001.
46. Sakurai, T.; Sugano, T. Theory of Continuously Distributed Trap States at $Si-SiO_2$ Interfaces. *J. Appl. Phys.* **1981**, *52*, 2889–2896.
47. Kayes, B. M.; Filler, M. A.; Putnam, M. C.; Kelzenberg, M. D.; Lewis, N. S.; Atwater, H. A. Growth of Vertically Aligned Si Wire Arrays Over Large Areas (> 1 cm^2) with Au and Cu Catalysts. *Appl. Phys. Lett.* **2007**, *91*, 103110.